16th World Conference on Earthquake, 16WCEE 2017
Santiago Chile, January 9th to 13th 2017
Paper N° 4073
Registration Code: S-J1464448052

COMPARISON OF LOSS ASSESSMENT USING REFINED ANALYSIS AND SIMPLIFIED DDBA APPROACH FOR AN EXISTING BUILDING IN ITALY

D. Saborío Romano[1], D.P. Welch[2], T.J. Sullivan [3], L. Landi [4]

[1] ROSE Programme, UME School, IUSS Pavia, Italy, daniel.saborio@umeschool.it
[2] ROSE Programme, UME School, IUSS Pavia, Italy, david.welch@umeschool.it
[3] Department of Civil and Natural Resources Engineering, University of Canterbury, Christchurch , New Zealand, timothy.sullivan@canterbury.ac.nz
[4] Department of Civil, Chemical, Environmental and Materials Engineering, University of Bologna, Bologna, Italy, l.landi@unibo.it

Abstract

The recently developed PEER Performance-Based Earthquake Engineering (PBEE) approach can be used to provide building owners and stakeholders with loss estimates, on which informed decisions can be made based on the likely performance of a building under seismic actions. The performance assessment procedure usually entails non-linear time history analyses of complex structural models, and subsequent evaluations of damage and losses, at multiple intensity levels, which requires considerable expertise and time. The motive of this work is to further the development and improvement of simplified assessment methods, that endeavor to provide reliable estimation of expected annual monetary losses stemming from earthquake induced damage to the building.

This study compares results from the seismic assessment of an existing building of reinforced concrete frames with masonry infill walls and partitions in L'Aquila, Italy, using the refined PEER methodology for PBEE and a simplified method, which applies concepts of Direct Displacement-Based Assessment (DDBA). The methodologies presented are targeted at predicting the performance of the structure under seismic actions at different intensity levels, in order to quantify the direct losses in economic terms. The research finds that generally, the expected annual losses predicted using the Direct DBA procedure are comparable with those predicted by the rigorous PEER PBEE approach.

Keywords: displacement-based assessment, simplified direct loss estimation, performance-based earthquake engineering.

1. Introduction

Traditionally, the Performance-Based Earthquake Engineering (PBEE) has been defined as a framework under which a desired structural system performance is sought for a specified seismic intensity level. Nowadays, the most advanced PBEE seismic assessment procedure appears to be the methodology developed by the Pacific Earthquake Engineering Research (PEER) Center [1], which leads to system performance measures, such as economic losses, downtime and casualties, these being parameters of interest for decision makers.

The PBEE PEER procedure consists of four successive stages of analysis: hazard analysis (site definition), structural analysis, damage analysis and loss (decision) analysis. In all the stages, the related uncertainties are explicitly considered in a probabilistic manner. Economic losses can be expressed in terms of a single intensity level, earthquake scenario (e.g. a given magnitude and distance case) or expressed in annualized terms (e.g. Expected Annual Loss) [2]; the latter of which is very attractive for decision makers since the entire hazard curve is considered (within reasonable bounds) and annualized values can be converted to present values to allow for cash flow analysis (i.e. cost-benefit analysis).

The PBEE PEER methodology usually requires the use of time-consuming and complex analysis procedures, this being the main reason for the development of simplified methods. The simplified loss estimation using Direct Displacement-Based Assessment (DDBA) concepts [3] is intended to achieve the aims of refined PBEE PEER methods (i.e. assist decision making), estimating the structural response without performing a series of Non-Linear Time History (NLTH) analysis, while providing an alternate means of defining capacity curve models for the simplified method of FEMA P-58 [2].

The basis of the DDBA loss model is the approximation of the mean annual frequency of exceedence (MAFE) versus Mean Damage Factor (MDF) (i.e. the expected economic loss) as a tri-linear curve, defined by four key limit states: zero loss, operational, damage control, and near collapse (refer to Fig.1). The zero loss limit state represents the beginning of the loss accumulation with a high MAFE, attributing a MDF value of 0.0. The operational and damage control limit states characterize the transition between significant MAFE and low loss to low MAFE and higher loss, where these points require an estimate of the corresponding MDF. The near collapse limit state has a low MAFE with a substantial loss accumulation, assuming a MDF value of 1.0 that represents the total replacement of the building; note that rare high intensity levels, despite significant losses, do not contribute significantly to Expected Annual Loss (EAL).

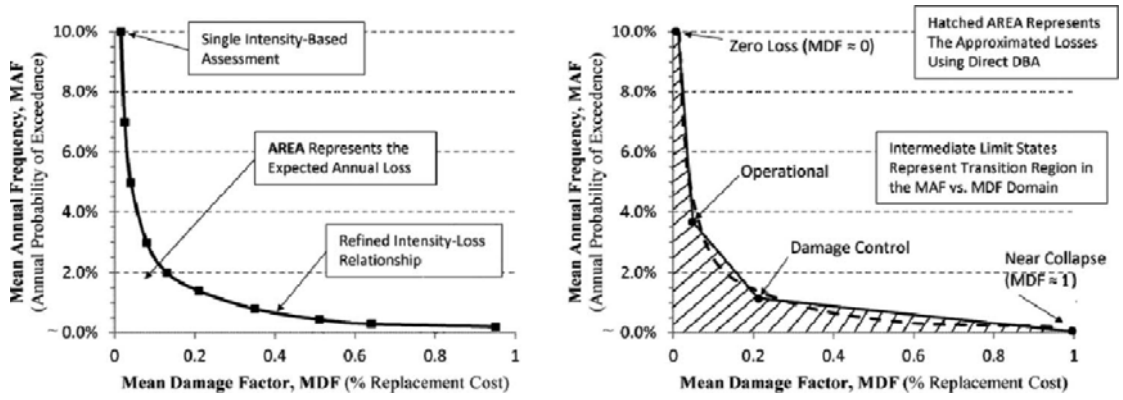

Fig. 1 – Comparison of expected annual loss calculation, using the PEER methodology (left) and the simplified Direct DBA loss estimation approach (right), taken from [3]

2. Case study building

The case study is an existing building of 6-storey RC frames with unreinforced masonry partitions and infill walls located in L'Aquila, in the central region of Italy. The building was damaged during the 2009 L'Aquila earthquake and subsequently retrofitted by the design office of Benedetti & Partners [4] in Bologna. The

building is regular in plan with 7 bays in the East-West direction (X direction) and 3 principal bays in the North-South direction (Y direction), with a total area per storey of 340.5m^2, as shown in Fig 2.

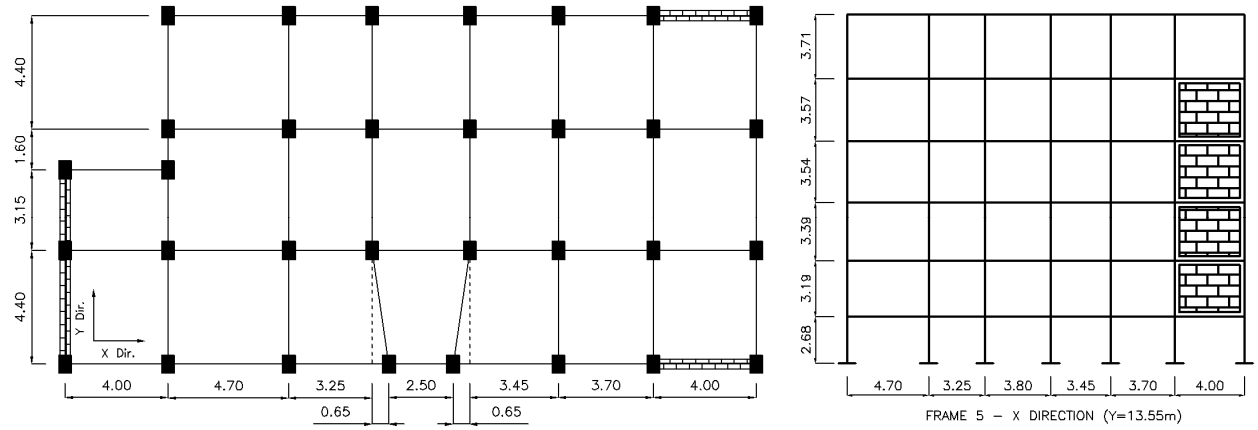

Fig. 2 – Plan view (left) and scheme of elevation for Frame 5 in East-West direction (right)

The first storey consists on a basement for wine cellars and storage rooms, separated from the perimeter retaining walls by a gap of 80cm. In the second storey are located offices, shops and garages and in the last four storeys are residential. The beam and column sections are gradually reduced from the lower to the upper storeys [4, 5], having continuity of the elements along the height. However, the storey heights increase from the lower to the upper storeys, causing an irregularity in the storey stiffness along the height.

Two different three-dimensional structural models were created using the software Ruaumoko 3D [6] namely: bare frame (BF) and infilled frame models (IF). The RC columns and beams were modeled as Giberson one-component members to create a lumped plasticity model, allowing plastic hinges formation on both ends of the elements, with the material properties and moment capacities described in [7]. The plastic hinges behavior was represented by adopting the modified "fat" and "thin" Takeda hysteresis rule, implemented in [6], for the beams and columns, respectively.

The contribution of the masonry infill walls (strength and stiffness) was considered only in the infilled frame model for walls that do not have any opening and were surrounded in all contact surfaces by a RC frame. The details of these walls are two 12cm thick solid clay brick leaves each separated by a center cavity of 14cm. The numerical model for these elements is two equivalent diagonal struts connected to the RC frames at the centerlines intersection, using a spring with the cyclic response of the Crisafulli hysteretic model [6]. The axial stress of these elements was derived from the lateral resistance forces model of [8] and the axial stiffness was obtained from the displacement-based model of [9]. The material properties of the masonry infill walls were assumed from [5] and the elements properties are described in [7]. Notably, adverse effects of frame-infill interaction (i.e. induced shear failures) are neglected in the structural model.

3. Structural analysis

Two different types of analyses were used to determine the structural response of the structure under seismic actions: Non-linear pushover and NLTH. In the pushover analysis the inelastic mechanism formation sequence and force-displacement curve were determined under a sustained monotonic inverse triangular lateral force vector. The limit states were defined according to the Italian code [10], in terms of the peak inter-storey drift at each storey, which are Operational (SLO), Damage Control (SLD), Life Safety (SLV) and Collapse Prevention (SLC) limit states. The capacity curves and the limit states considered for both directions are shown in Fig.3.

The NLTH analyses were performed to obtain reliable structural response quantities (i.e. EDPs) under a suite of selected ground motions for the building site. The hazard information for L'Aquila was obtained with a Probabilistic Seismic Hazard Assessment (PSHA) conducted by [11], on which the selection of the ground motions was made. The Uniform Hazard Spectra (UHS) for nine intensity levels, illustrated in Fig.4a, are

defined in terms of their probability of exceedence in 50 years according to [12]. The period of interest for the building is taken as 1.5s, being the closest available value between the initial period of the two structural models ($T_{1,X}$=1.83s and $T_{1,Y}$=1.43s for the BF and $T_{1,X}$=1.41s and $T_{1,Y}$=1.21s for the IF) and the natural periods of the UHS of L'Aquila. The hazard curve at this period of interest is shown in Fig.4b.

The ground motions were selected from the catalogue of [13] and scaled following the procedure of [14] to be compatible with the conditional spectra for the site (conditioned at T=1.5s), using the maximum spectral acceleration of the two orthogonal components of the record. A total of ninety records were selected and used to perform these analyses, and the EDPs obtained are described in [7].

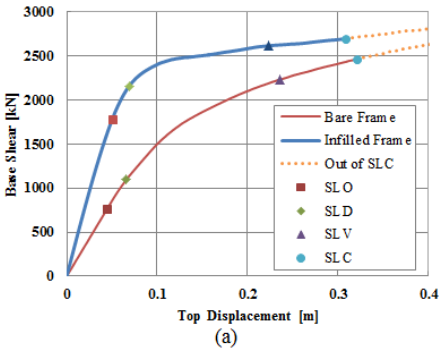

(a)

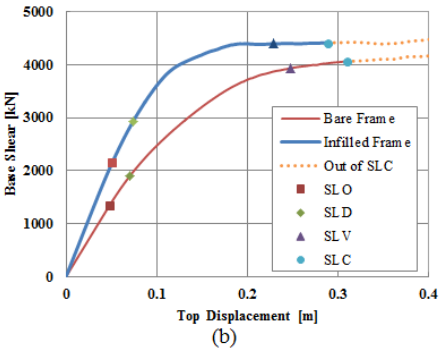

(b)

Storey	SLO θ [rad]	SLD θ [rad]	X direction SLV θ [rad]	X direction SLC θ [rad]	Y direction SLV θ [rad]	Y direction SLC θ [rad]
1st	0.003	0.005	0.0156	0.0209	0.0147	0.0196
2nd			0.0166	0.0221	0.0166	0.0221
3rd			0.0177	0.0236	0.0177	0.0236
4th			0.0197	0.0263	0.0182	0.0243
5th			0.0203	0.0271	0.0203	0.0271
6th			0.0219	0.0292	0.0219	0.0292

(c)

Fig. 3 – Capacity curve in (a) X and (b) Y directions and (c) the limit states defined by the Italian Code [10]

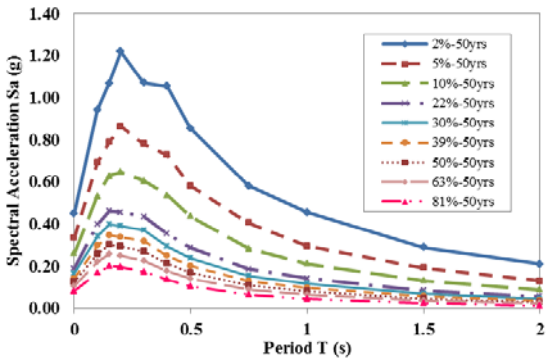

(a)

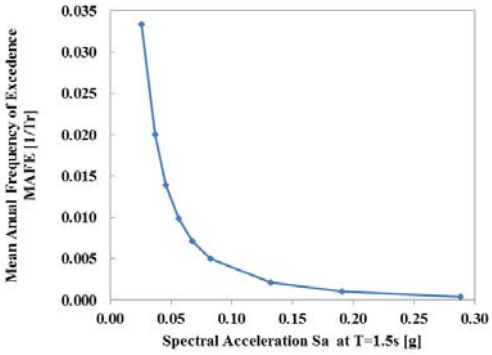

(b)

Fig. 4 – Site hazard information for L'Aquila

4. Refined loss analysis

The loss analysis performed was executed using the Performance Assessment Calculation Tool (PACT) software, presented in the FEMA P-58 guidelines [15] and it was based only on the economic loss due to damage of the building components; neglecting casualties or downtime losses. The total replacement cost of the building was assumed as 3.064.500€, considering a replacement cost per square meter of 1.500€. The core and shell replacement cost was considered as 1.500.000€, which is the restoration value of retrofitting determined by [4].

4.1 Damage analysis

The most-likely damage that could occur in a component of case study building is carried out through fragility functions. For the RC frame and elevator components of the building, the default fragility functions described in Table 1 were selected from the library of PACT [15], while for the glazing windows and masonry components (infill walls and partitions) the fragility curves and repair costs of [16] and [9] were selected, respectively, consistent with the type of elements and construction practice in Italy. Additionally, a default building residual drift fragility curve provided in PACT [15] was selected to determine if the repair of the building is practical

with the residual deformation after the seismic actions. Table 1 presents the damageable assemblies with the corresponding fragility functions, unit quantities and repair cost considered for each component type.

Table 1 – Damageable components and corresponding fragility functions, unit quantities and repair cost

					Quantities X:# in X dir., Y:# in Y dir. ND:# in Non-Directional							
Description	Damage State	EDP	EDP_{med}	β	Unit	1st St.	2nd St.	3rd St.	4th St.	5th St.	6th St.	Repair Cost [€ per unit]
Windows 1.0x1.0m	DS0	IDR*	0.0025	0.30	ea.	-	X:5	X:2	X:2	X:2	-	10
	DS1	IDR	0.0224	0.30								190
	DS2	IDR	0.0244	0.30								52
Windows 1.0x2.5m	DS0	IDR	0.001	0.30	ea.	-	-	X:3 Y:1	X:3 Y:1	X:3 Y:1	X:3 Y:1	10
	DS1	IDR	0.0153	0.30								265
	DS2	IDR	0.0184	0.30								1151
Windows 1.5x1.5m	DS0	IDR	0.001	0.30	ea.	-	-	X:14	X:13 Y:3	X:13 Y:3	X:9	10
	DS1	IDR	0.0136	0.30								250
	DS2	IDR	0.0148	0.30								1045
Windows 1.0x0.5m	DS0	IDR	0.0005	0.30	ea.	-	-	Y:5	X:3 Y:3	X:3 Y:3	X:1 Y:5	10
	DS1	IDR	0.0279	0.30								164
	DS2	IDR	0.0148	0.30								309
Masonry partitions	DS1	IDR	0.0014	0.36	m^2	X:66 Y:90	X:79 Y:107	X:83 Y:114	X:87 Y:119	X:88 Y:120	X:95 Y:130	62.9
	DS2	IDR	0.0033	0.48								142.4
	DS3	IDR	0.0096	0.21								296.5
	DS4	IDR	0.02	0.28								476.3
Masonry infill walls	DS1	IDR	0.0014	0.36	m^2	X:118 Y:60	X:122 Y:63	X:130 Y:67	X:136 Y:69	X:137 Y:70	X:149 Y:76	62.9
	DS2	IDR	0.0033	0.48								142.4
	DS3	IDR	0.0096	0.21								296.5
	DS4	IDR	0.02	0.28								476.3
RC Non-conforming MF, beam one side (B1014.111a)	DS1	IDR	0.015	0.40	ea.	X:10 Y:16	X:10 Y:16	X:10 Y:16	X:10 Y:16	X:10 Y:16	X:10 Y:16	Cost functions defined in PACT [15] library
	DS2	IDR	0.02	0.40								
	DS3	IDR	0.025	0.40								
RC Non-conforming MF, beam both side (B1014.111b)	DS1	IDR	0.015	0.40	ea.	X:22 Y:16	X:22 Y:16	X:22 Y:16	X:22 Y:16	X:22 Y:16	X:22 Y:16	
	DS2	IDR	0.02	0.40								
	DS3	IDR	0.025	0.40								
Elevator (D1014.012)	DS1	PGA**	0.31	0.45	ea.	ND:1	-	-	-	-	-	
Residual Drift	DS1	R-IDR***	0.01	0.3	ea.	ND:1	-	-	-	-	-	TRC****

*IDR= Inter-Storey Drift Ratio, **PGA=Peak Ground Acceleration, ***R-IDR= Residual Inter-Storey Drift Ratio, ****TRC=Total Replacement Cost

4.2 Loss estimation results

The economic losses obtained are reported as the EAL and 4 intensity-based assessments at 81%, 63%, 10% and 5% probability of exceedance in 50 year hazard levels were selected based on the limit states considered by the Italian Code [10] to show the variation in the results with increasing seismic demands. Additionally a sensitivity analysis was performed in order to evaluate the change in the loss estimation with different assumptions done in the damage analysis, which are described as follows:

- Basic model: model based on the fragility functions and repair cost information previously described. Models are referred to as BF.1 and IF.1.
- Variation in damage states of RC columns: The median drifts corresponding to DS2 and DS3 for RC columns are taken as the limit states SLV and SLC (refer to Fig 3) of the Italian Code [10], respectively. In the first models, referred to as BF.2 and IF.2, the DS3 is changed to the limit state SLC, while in the models BF.3 ad IF.3 the damage state DS2 is taken also as the limit state SLV.

- Variation on the residual drift fragility function: The median value of the default fragility curve of PACT [15] for residual drift was changed to 1.2% in the models BF.4 and IF.4, and 0.8% in the models BF.5 and IF.5. The dispersion was kept at the default value of 0.3 provided in PACT [15].

A summary of the median repair cost estimates for each model is shown in Table 2, while Fig.5 illustrates the influence of the components in the losses obtained for the intensity levels considered in the basic models.

Table 2 – Comparison of key loss metrics for models, including variations of parametric study

Model		BF.1	BF.2	BF.3	BF.4	BF.5	IF.1	IF.2	IF.3	IF.4	IF.5
EAL € [%]		9368 [0.306%]	9440 [0.308%]	9450 [0.308%]	9389 [0.306%]	9349 [0.305%]	7719 [0.252%]	7793 [0.254%]	7825 [0.255%]	8110 [0.265%]	7218 [0.236%]
Annualized Probability to Complete Loss due to Residual Drift [%]		0.0235%	0.0235%	0.0235%	0.0251%	0.0219%	0.0569%	0.0569%	0.0569%	0.0842%	0.0366%
Losses at limit states of NTC2008 € [%]	81% in 50yrs (SLO)	57600 [1.88%]					22600 [0.74%]				
	63% in 50yrs (SLD)	103462 [13.5%]					61500 [8.38%]				
	10% in 50yrs (SLV)	390000 [12.73%]					350000 [11.4%]				
	5% in 50yrs (SLC)	1577500 [51.5%]	1700000 [55.5%]	1705000 [55.6%]	1600000 [52.2%]	1572500 [51.3%]	1025000 [33.4%]	1045000 [34.1%]	1050000 [34.3%]	1035000 [33.8%]	970000 [31.7%]

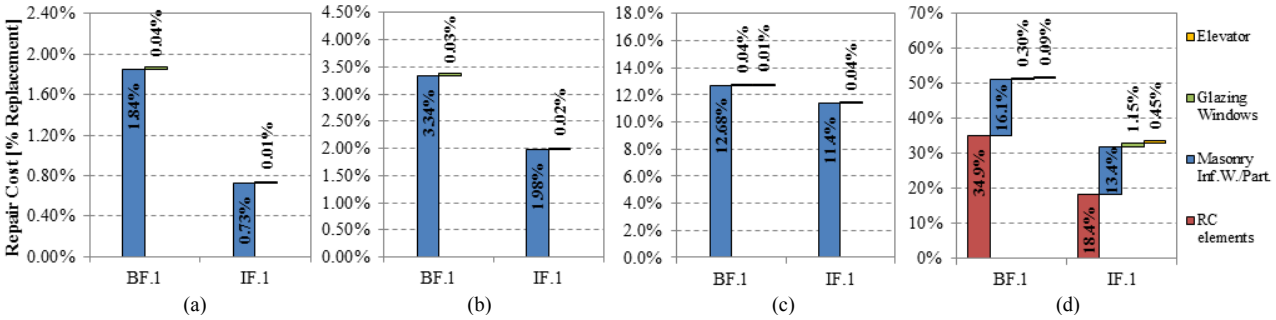

Fig. 5 – Influence of the components on the repair cost at intensity level of (a) 81% in 50 years, (b) 63% in 50 years, (c) 10% in 50 years and (d) 5% in 50 years, with the EDPs of the NLTH analysis of BF and IF models

As shown in Table 2, for the basic models the largest losses are obtained for the BF model, with an EAL of 0.306%, where the masonry infill walls were not considered in the structural analysis but were still included in the repair cost analysis. For the IF model, where the infill walls were accounted for in the structural response, the EAL has a value of 0.252%. These results show the variation on the EAL by considering or not the masonry infill walls as part of the structural system during the analysis phase. It is also seen in Fig.5 that the highest contributor to economic losses in the lower three intensity levels is damage on the masonry infill walls and partitions, while for the higher intensity level masonry infills become the second most important contributor to losses. These results, in addition to the corresponding MAFE at the intensity levels (higher MAFE in the lower intensity levels and vice versa), confirm that masonry components are significant to the loss analysis results.

The results of the sensitivity analysis also indicate a small variation in the EAL value due to different assumptions of the RC elements' damage states and the building residual drift fragility curve. This result shows that the default fragility curves selected for the RC columns are in accordance with the SLV and SLC limit states of the Italian Code [10] and that the residual drifts obtained, due to the structure response under the seismic actions, do not have a strong influence in the loss estimation for the current case study. The only variation in the repair cost due to the changes of the sensitivity analysis is apparent at the largest intensity level (see Table 2) but the MAFE associated to this level is small, obtaining the same EAL in practical terms as the basic models.

5. DDBA of the case study building

The application of the DDBA procedure for the case study building is developed in this section, using the traditional displaced shape for RC frames, proposed by [17], and the new displaced shape for assessment, developed by [7]. Additionally the results obtained are compared with the non-linear pushover analysis to validate them and obtain the EDPs for the DDBA simplified loss estimation of [3].

The initial step of the DDBA is the determination of the most likely inelastic mechanism of the building to develop. For RC frame structures, [17] proposed a sway potential index S_i for each storey, relating the relative strengths of the beams and columns according to Eq. (1):

$$S_i = \frac{\sum_j M_{bl} + M_{br}}{\sum_j M_{ca} + M_{cb}} \tag{1}$$

where the terms M_{bl} and M_{br} are the expected beam flexural strengths at the left and right of the joint j, respectively, and M_{ca}, M_{cb} are the expected column flexural strengths above and below the joint j. Moment capacities at the face of the joint are then extrapolated to the joint centroid. The column moment capacities are determined using the gravity axial load, neglecting the variation of the axial force due to seismic action, as suggested by [17]. The beam and column moments are summed over the total of joints j in the frames of the analysis direction at the floor level i. When S_i is greater than 1.0 a column-sway mechanism is expected in the storey, while if S_i is lower than 0.85 a beam-sway mechanism is assumed. When S_i is less than 1.0 a beam-sway mechanism could be expected, but [17] point out that if S_i is greater than 0.85 then it would be prudent to assume a column-sway mechanism. The resulting sway potential indices, shown in [7], suggest that a beam-sway mechanism is likely to develop in all storeys in both directions, except in the last storey where the sway potential indices are higher than 1.0, predicting a column-sway mechanism at the roof level, however the hinging of the columns at that level does not imply a soft-storey, being acceptable within common design practice.

Knowing that the beam-sway mechanism is expected, for the assessment of the case study the transition from the linear to non-linear range of the capacity curve was obtained by assessing the frames at the development of the expected yield drift at each storey until the full mechanism was developed. In order to determine the storey displacement ductility μ_i, the yield drift $\theta_{y,i}$ per storey i is estimated through a weighted average based on the moment capacity $M_{j,I}$ and the yield drift θ_y of the beam j, for an irregular RC frame configuration (i.e. different beams lengths and heights), with Eq. (2).

$$\theta_y = 0.5\varepsilon_y \frac{L_b}{h_b} \rightarrow \theta_{y,i} = \frac{\sum_j M_{j,i}\theta_{y,j,i}}{\sum_j M_{j,i}} \rightarrow \mu_i = \frac{\theta_i}{\theta_{y,i}} \tag{2}$$

Associated with the development of the expected yield drift on each storey, the yield shear per storey $V_{y,i}$ is obtained by summing up the shear expected in the columns with the predicted mechanism, through the moments in the top $M_{col,top,i,j}$ and bottom $M_{col,bot,i,j}$ part of the column j in the storey i that can be developed after reaching joint equilibrium. The moments at joint equilibrium are taken as the minimum between the sum of the column moments and beam moments extrapolated to the joint centroid as well as the moment resistance of the joint itself. Then the overturning moment OTM capacity of the structure is obtained by adding the yield shear-storey height pair, shown in Eq. (3).

$$V_{y,i} = \frac{\sum_j M_{col,top,i,j} + \sum_j M_{col,bot,i,j}}{h_{s,i}} \rightarrow OTM = \sum_{i=1}^{n} V_{y,i} \cdot h_{s,i} \tag{3}$$

The displacement profile Δ_i, proposed by [17] is estimated by using a normalized inelastic first mode shape, for a predicted beam-sway mechanism and the magnitude of the displacement is governed by the inter-

storey drift θ_c at the critical storey (typically assumed at the first storey for beam-sway). The displacement at the critical storey is related to those of the remaining storeys through Eq. (4) for buildings with more than 4 storeys, which depends on the number of storeys n, height of the storey H_i, roof height H_n and height at critical storey H_c. The higher mode factor ω_θ, for this case study is estimated and considered as 1.

$$\delta_i = \frac{4}{3}\left(\frac{H_i}{H_n}\right)\left(1-\frac{H_i}{4H_n}\right) \rightarrow \Delta_i = \omega_\theta \theta_c H_c \frac{4H_n - H_i}{4H_n - H_c} \quad (4)$$

Nevertheless, the displaced shape recommended by [17] assumes the plastic hinge formation at column base level and the relative stiffness between adjacent floors are very similar, which is not necessarily accurate for existing buildings, as is the situation for the case study. For this reason, [7] proposed a new displaced shape for RC frames considering the relative stiffness of the storeys; the variation of yield drifts between adjacent floor levels and the yield drift of the columns at the base level. Additionally, in order to account the contribution of the masonry infill walls in the capacity curve in the IF model, the procedure by [7] is used, which consists in the use of the displaced shape obtained for the bare frame, considering the masonry infill walls only for the *OTM* resistance of the structure.

Fig.6 illustrates the comparison between the 1st mode shape obtained with the BF model, the traditional displacement profile (see Eq. (4)) and elastic displaced shape obtained with the new approach of [7] for RC frames. It is apparent that the new procedure works much better for the frame system in question; for further details of the procedure, refer to [7].

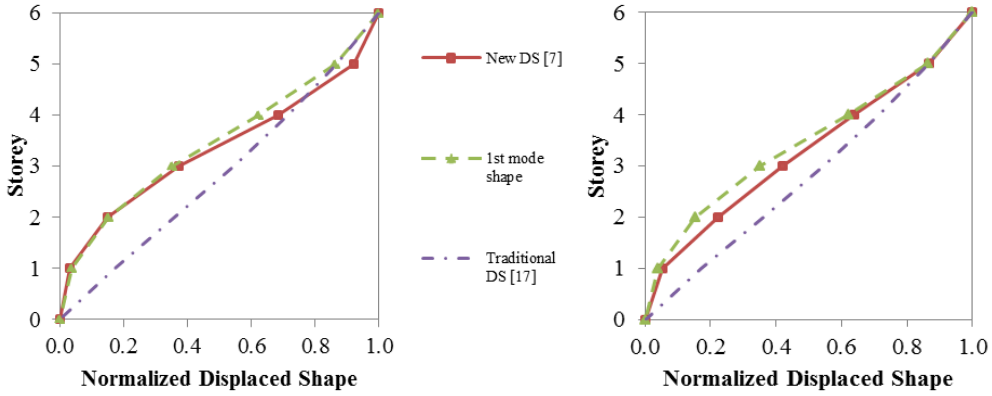

(a) (b)

Fig. 6 – Comparison of the new displaced shape proposed by [7], the 1st mode shape and the traditional displacement profile of [17], for the bare frame model in (a) X and (b) Y directions

After the displaced shape is obtained, the equivalent single degree of freedom (SDOF) structure transformation is obtained following the substitute structure concepts of [18, 19], through the SDOF parameters shown in Eq. (5). With the mass per storey m_i, the displacement profile Δ_i and the expected *OTM* of the structure, the SDOF displacement capacity Δ_{cap}, effective mass m_e, effective height H_e, equivalent base shear V_{base}, effective stiffness k_e and effective period T_e are calculated.

$$\Delta_{cap} = \frac{\sum m_i \Delta_i^2}{\sum m_i \Delta_i} \quad m_e = \frac{\left(\sum m_i \Delta_i\right)^2}{\sum m_i \Delta_i^2} \quad H_e = \frac{\sum m_i \Delta_i H_i}{\sum m_i \Delta_i} \quad V_{base} = \frac{OTM}{H_e} \quad K_e = \frac{V_{Base}}{\Delta_{cap}} \quad T_e = 2\pi\sqrt{\frac{m_e}{K_e}} \quad (5)$$

In Fig.7 is shown a comparison of the force-displacement response obtained for structural models BF and IF and the SDOF transformation obtained with the DDBA concepts using the traditional displaced shape and the new displaced shape formulation. From Fig.7 it can be seen that the capacity curves based on the new displaced shape predicted with better results the force-displacement relationship, compared to the results obtained with the traditional displaced shape. The overestimation of the capacity curve of the BF model using the traditional displaced shape is mainly due to the assumption of plastic hinge formation at column base level and in all beams

along height. In the pushover results, the inelastic mechanism obtained did not have any hinging at column base level nor in the first two and the last storeys, the beams developed very few plastic hinges, which can be seen in detail in [7]. For the BF model in the X direction, the anticipated capacity curve tends to have a lower stiffness in the elastic branch and the transition between elastic-inelastic behavior is nicely captured with the new displacement profile used. In the Y direction for the BF model, the initial stiffness and the elastic-inelastic transition shape are similar to the structural model curve; however the elastic branch is longer. On the other hand, for the IF model the capacity curves obtained show good results, capturing the overall behavior of the structure, with a good estimation of the elastic branch and a slight overestimation of the shear resistance at ultimate capacity. The transition between the elastic-inelastic behavior in the X direction is slight underestimated, while for the Y direction is slightly overestimated. In all cases, the overestimation of the base shear is lower than 14.0%.

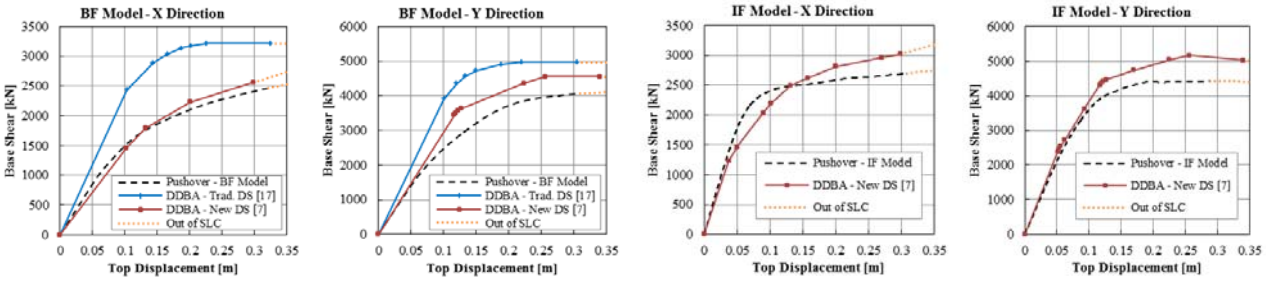

Fig. 7 – Comparison of the capacity curve of the SDOF system with the new displaced shape proposed by [7] and the traditional displacement profile of [17], for both models in both directions

In order to apply the PEER PBEE approach using the DDBA simplified loss approach, the capacity curves obtained are converted to spectral acceleration-displacement (i.e. ADRS format) curves. For the BF model, the inelastic spectra is constructed following the procedure of [20], considering the variation of the system ductility demand μ with the period T_i from the original period T_e and with a post-yield stiffness ratio r (typically 0.05 for RC structures). Also, as recommended by [20], the effects of inelastic response and energy dissipation are accounted through an equivalent viscous damping (EVD) ξ_{eq} and then a spectral scaling factor η modifies the elastic spectra to obtain the inelastic spectra. All these parameters are estimated using Eq. (6).

$$\mu = \frac{\left(\frac{T_e}{T_i}\right)^2 (1-r)}{\left(1-r\left(\frac{T_e}{T_i}\right)^2\right)} \rightarrow \xi_{eq,RC\cdot frame} = 0.05 + 0.565\left(\frac{\mu-1}{\mu\pi}\right) \; for\; \mu \geq 1 \rightarrow \eta = \left(\frac{0.07}{0.02+\xi_{eq}}\right)^{0.5} \quad (6)$$

For the IF model, the equivalent viscous damping $\xi_{eq,syst}$ is obtained with a weighted average based on the energy dissipated by the different structural elements at each storey $\xi_{eq,i}$, as shown in Eq. (7), using the storey displacement ductility demand μ_i of Eq. (2). For the RC frame, the EVD is estimated with Eq. (6) and for the masonry infill walls, two approaches were used: the EDV expression of [21], shown in Eq. (6) and 10% of EVD due to hysteretic response, based on experimental information [22, 23]. These two approaches are referred in this study as EVD1 and EVD2, respectively.

$$\xi_{eq,Infill\cdot frame} = 0.05 + 0.83\left(\frac{\mu-0.07}{\mu\pi}\right) \; for\; \mu \geq 0.07 \rightarrow \xi_{eq,syst} = \frac{\sum V_i\theta_i\xi_{eq,i}}{\sum V_i\theta_i} \quad \eta = \left(\frac{0.07}{0.02+\xi_{eq}}\right)^{0.5} \quad (7)$$

6. Simplified DBA Loss Estimation

The loss estimation results for the case study are obtained using the DDBA simplified approach [3], where the EDPs for both directions are calculated only on the two selected intermediate intensity level, assuming them as

the median response values with dispersion factors estimated according to [2] and accounted for in the loss analysis. With the assumptions on the two bounding limit states, the tri-linear loss curve is obtained, performing only the loss estimations at two intermediate points to obtain the EAL estimate. In order to estimate the individual inter-storey drift profile for the two intermediate intensity levels, the system displacement capacity Δ_{cap} of Eq. (5) is equated to the spectral displacement obtained with the inelastic spectra considering the displaced shape used and a multiplier factor obtained in an iterative process. Then with the displacement profile Δ_{cap}, the inter-storey drift is obtained dividing the displacement with the storey height.

6.1 Definition of key limit states

In order to implement the simplified tri-linear loss model, the MDF in the two intermediate limit states requires to be quantified for EAL calculation, while for the bounding limit states, the assumptions shown in section 1 were made. The operational limit state is considered as peak inter-storey drift of 0.33%, being this value the damage state DS2 of the masonry infill walls, which according to [9], below this value some repairs will be necessary, however, not leading to significant repair effort or disruption in the facility, following the recommendation of [3]. For the damage control limit state, [3] suggests to consider this threshold as the first yielding of any storey, being the first transition point from linear to non-linear behavior in the capacity curve. From the results shown in [7], this transition in the capacity curve occurs at the 10% in 50years intensity level for both models, having a peak inter-storey drift of 0.92% in the 4th storey, overpassing the yield threshold of 0.896% shown for that storey in Fig.3.

6.2 Estimation of dispersion in demand and capacity

Knowing that the DDBA simplified approach only requires a single vector of EDPs for each direction and intensity level, the influence of uncertainties are accounted with the approach of [2], which attributes to the median inter-storey drift and floor acceleration responses (estimated using the approach described in [2]) the total dispersion factors β_{SD} and β_{FA}, respectively, as shown in Eq. (8) and (9):

$$\beta_{SD} = \sqrt{\beta_{a\Delta}{}^2 + \beta_m{}^2} \tag{8}$$

$$\beta_{FA} = \sqrt{\beta_{aa}{}^2 + \beta_m{}^2} \tag{9}$$

where $\beta_{a\Delta}$ and β_{aa} are the analysis record-to-record dispersion for drift and accelerations respectively, which consider random uncertainty in the seismic demands, and β_m is the modelling dispersion that incorporates the uncertainty related of the structural response. These three dispersion factors are taken from [2].

6.3 DDBA loss estimation results using the simplified approach

Table 3 presents the four points considered for the tri-linear EAL curve based on the limit states and the EAL values obtained with the refined loss analysis and the one found with the simplified approach for both models.

Table 3 - Four limit states considered for tri-linear EAL curve and EAL value using DDBA simplified loss estimation of [3]

	Bare Frame (BF)		
Limit states for Tri-linear curve	Int. Level	MAFE	Economic Loss [€]
Zero-Loss	81% in 50yr	0.0333	0
Operational	50% in 50yr	0.0139	127941
Damage Control	10% in 50yr	0.0021	377500
Near Collapse	2% in 50yr	0.0004	3064500

	Infilled Frame (IF)			
Int. Level	MAFE	Economic Loss [€]		
		EVD1	EVD2	
81% in 50yr	0.0333	0	0	
22% in 50yr	0.0050	131875	156667	
10% in 50yr	0.0021	249412	289167	
2% in 50yr	0.0004	3064500	3064500	

	EAL € [%]
Refined BF	9368 [0.306%]
DDBA BF	8388 [0.274%]
Refined IF	7719 [0.252%]
DDBA IF-EVD1	6474 [0.211%]
DDBA IF-EVD2	6952 [0.227%]

From Table 3, the EAL for the BF model obtained using the DDBA simplified approach has a value of 0.274%, being 0.895 times the EAL of the refined loss assessment, showing a great prediction of this parameter. For the IF model, the EAL obtained for damping approaches EVD1 and EVD2 are 0.211% and 0.227%, which are 0.853 and 0.901 times the EAL obtained with the refined loss analysis. These results show that the DDBA

simplified loss estimation gives reasonable loss approximations, being for all cases the EAL lower than the value obtained with the refined loss model. Comparing the two damping approaches for the IF model, the damping approach EVD1 could lead to lower EAL values due to a higher over-damping of the seismic response of the structure in comparison with the EVD2 approach, so for a simplified loss analysis of an infilled frame structure, the EVD2 method could be used leading to a good estimation of economic losses.

7. Conclusions

The DDBA simplified loss estimation approach of [3] can provide a good estimation of the expected annual losses (EAL), when an appropriate displaced shape is used to determine the capacity of the structure in terms of displacements and base shear. The use of the new displaced shape, proposed by [7], seems more suitable in seismic assessment of existing buildings, especially if the structures do not possess modern seismic design concepts in their details. Additionally, it's important to appropriately select the two intermediate limit states of the simplified tri-linear curve because the loss estimation of the structure is based on the results obtained in these intensity levels. The simplified DDBA loss analysis applied gives an EAL lower than the one obtained with the refined loss assessment for the two models considered. However, the value found is considered a good approximation, being an acceptable range for a quick loss analysis, without the use of computer structural models and complex analysis.

8. Acknowledgements

The funding provided by the RELUIS consortium as part of the 2016 RELUIS project is gratefully acknowledged.

9. References

[1] Porter KA (2003): An Overview of PEER's Performance-Based Earthquake Engineering Methodology. *Proceedings of Ninth International Conference on Applications of Probability and Statistics in Engineering*, San Francisco, California, USA.

[2] FEMA P-58 (2012a): *Seismic Performance Assessment of Buildings: Vol. 1 – Methodology, FEMA P-58-1*, Prepared by the Applied Technology Council for the Federal Emergency Management Agency, Washington, D.C, USA.

[3] Welch DP, Sullivan TJ, Calvi GM (2014): Developing Displacement-Based Procedures for Simplified Loss Assessment in Performance-Based Earthquake Engineering. *Journal of Earthquake Engineering*, **18** (2), 290-322.

[4] Benedetti A (2011): Interventi di Miglioramento Sismico – Condominio "D'Annunzio" via D'Annunzio, 8 L'Aquila, *Benedetti & Partners: Studio Associato di Ingegneria*, Bologna, Italy.

[5] Gilberti S (2015): Performance based assessment of a RC frame building in L'Aquila, *Dissertation*, European School for Advanced Studies in Reduction of Seismic Risk (ROSE School), University of Pavia, Pavia, Italy.

[6] Carr AJ (2013): *RUAUMOKO Inelastic Time-History Analysis of Three-Dimensional Framed Structures, University of Canterbury*, Christchurch, New Zealand.

[7] Saborío Romano D (2016): Performance-Based and Simplified Displacement-Based Assessments of an Infilled RC Frame Building in L'Aquila, Italy, *Dissertation*, European School for Advanced Studies in Reduction of Seismic Risk (ROSE School), University of Pavia, Pavia, Italy.

[8] Decannini L, Mollaioli F, Saragoni R (2004): Seismic performance of masonry infilled RC frames, *13th World Conference on Earthquake Engineering*, No. 165, Vancouver, Canada.

[9] Sassun KP, Sullivan TJ, Morandi P, Cardone D (2016): Characterizing the In-Plane Seismic Performance of Infill Masonry, *Bulletin of the New Zealand Society for Earthquake Engineering*, in press.

[10] NTC (2008): *Norme Tecniche per le Construzioni, decreto 14 febbragio 2008*, Ministero delle Infrastrutture, Roma, Italy.

[11] Montaldo V, Meletti C (2007): *Valutazioni di ag (16mo, 50mo e 84mo percentile) con le seguenti probabilità di superamento in 50 anni: 81%, 63%, 50%, 39%, 30%, 22%, 5%, 2%, rispettivamente corrispondenti a periodi di ritorno di 30, 50, 72, 100, 140, 200, 1000 e 2500 anni.,* Istituto Nazionale di Geofisica e Vulcanologia, Milano, Italy.

[12] Montaldo V, Meletti C (2007): *Valutazione del valore della ordinata spettrale a 1 sec e ad altri periodi di interesse ingegneristico*, Istituto Nazionale di Geofisica e Vulcanologia, Milano, Italy.

[13] SHARE (2013): *EU-FP7 project: Seismic Hazard Harmonization in Europe*, Collaborative Project coordinated by the Swiss Seismological Service, Zurich, Switzerland.

[14] Ay BÖ, Fox MJ, Sullivan TJ (2016): Practical challenges facing the selection of conditional spectrum-compatible accelerograms, *Journal of Earthquake Engineering*, in press.

[15] FEMA P-58 (2012): *Seismic Performance Assessment of Buildings: Vol. 2 – Implementation Guide, FEMA P-58-2*, Prepared by the Applied Technology Council for the Federal Emergency Management Agency, Washington, D.C., USA.

[16] Sassun KP (2014): A Parametric Investigation into the Seismic Behaviour of Window Glazing Systems, *Dissertation*, European School for Advanced Studies in Reduction of Seismic Risk (ROSE School), University of Pavia, Pavia, Italy.

[17] Priestley MJN, Calvi GM, Kowalsky MJ (2007): *Displacement Based Seismic Design of Structures*, IUSS Press, Pavia, Italy.

[18] Gulkan P, Sozen MA (1974): Inelastic Response of Reinforced Concrete Structures to Earthquake Motions, *ACI Journal*, **71** (12), 604-610.

[19] Shibata A, Sozen MA (1976): Substitute Structure Method for Seismic Design in Reinforced Concrete, *Journal of the Structural Division*, ASCE, **102** (1), 1-18.

[20] Sullivan TJ, Welch DP, Calvi GM (2014): Simplified Seismic Performance Assessment and Implications For Seismic Design, *Earthquake Engineering and Engineering Vibration*, **13** (1), 95-122.

[21] Landi L, Benedetti A (2013): *Reinforced Concrete Buildings, Chapter 3 in Developments in the Field of Displacement-Based Assessment*, Edited by Sullivan TJ and Calvi GM, IUSS Press, Pavia, Italy.

[22] Morandi P, Hak S, Magenes G (2014): In-plane Experimental Response of Strong Masonry Infills, *9th International Masonry Conference*, International Masonry Society, Guimarães, Portugal.

[23] Ozkaynak H, Yuksel E, Yalcin C, Dindar AA, Buyukozturk O (2014): Masonry infill walls in reinforced concrete frames as a source of structural damping, *Earthquake Engineering & Structural Dynamics*, **43** (9), 949–968.